ISSN 0021-3640, JETP Letters, 2017, Vol. 105, No. 10, pp. 651–656. © Pleiades Publishing, Inc., 2017.
Original Russian Text © V.G. Myagkov, L.E. Bykova, V.Yu. Yakovchuk, A.A. Matsynin, D.A. Velikanov, G.S. Patrin, G.Yu. Yurkin, G.N. Bondarenko, 2017, published in Pis'ma v Zhurnal Eksperimental'noi i Teoreticheskoi Fiziki, 2017, Vol. 105, No. 10, pp. 610–615.

CONDENSED MATTER

High Rotatable Magnetic Anisotropy in MnBi Thin Films

V. G. Myagkov[a, *], L. E. Bykova[a], V. Yu. Yakovchuk[a], A. A. Matsynin[a], D. A. Velikanov[a], G. S. Patrin[a, b], G. Yu. Yurkin[a, b], and G. N. Bondarenko[c]

[a] *Kirensky Institute of Physics, Federal Research Center Krasnoyarsk Scientific Center, Siberian Branch, Russian Academy of Sciences, Krasnoyarsk, 660036 Russia*

[b] *Siberian Federal University, Krasnoyarsk, 660041 Russia*

[c] *Institute of Chemistry and Chemical Technology, Federal Research Center Krasnoyarsk Scientific Center, Siberian Branch, Russian Academy of Sciences, Krasnoyarsk, 660049 Russia*

**e-mail: miagkov@iph.krasn.ru*

Received April 10, 2017

The variations of the structural and magnetic properties of Bi/Mn/Bi and Mn/Bi/Mn trilayer film systems of equiatomic composition in the process of vacuum annealing are studied. The annealing of Bi/Mn/Bi films at a temperature of 270°C for an hour results in the synthesis of the well-studied highly oriented low-temperature LT-MnBi(001) phase with the perpendicular magnetic anisotropy $K_u \sim 1.1 \times 10^7$ erg/cm^3 and coercivity $H_C \sim 1.5$ kOe. In contrast to Bi/Mn/Bi, polycrystalline LT-MnBi nanoclusters are formed in Mn/Bi/Mn films under the same annealing conditions. A high rotatable magnetic anisotropy exceeding the shape anisotropy is detected in the films under consideration: the easy axis of anisotropy with the inclusion of the delay angle in magnetic fields above the coercivity $H > H_C = 9.0$ kOe can be oriented in any spatial direction. It is shown that the nature of rotatable magnetic anisotropy is due to the structural coexistence of epitaxially coupled LT-MnBi and QHTP-$Mn_{1.08}$Bi phases. The reported experimental results indicate the existence of a new class of ferromagnetic film media with the spatially tunable easy axis.

DOI: 10.1134/S0021364017100095

INTRODUCTION

The ferromagnetic properties and production of MnBi intermetallic compounds are widely used as a possible alternative to rare-earth metals in the production of permanent magnets [1–4] and film magnetic media for magnetic optical recording [5–7]. One of the main components of MnBi magnetic compounds is the low-temperature LT-MnBi phase, which has a high anisotropy, relatively high magnetization, and large Faraday rotation [5–7]. With an increase in the temperature above 633 K (360°C), the LT-MnBi phase is transformed to a HTP-MnBi high-temperature paramagnetic phase, which is transformed to a QHTP-$Mn_{1.08}$Bi ferromagnetic phase at fast quenching. The quenched QHTP-$Mn_{1.08}$Bi phase is thermally unstable and is slowly transformed in two years to a stable LT-MnBi phase [7]. It is assumed that this transition occurs through unknown metastable phases [8–10], including a quasicrystalline phase [11]. Although ab initio calculations imply the stabilization of the LT-MnBi structure at the partial substitution of other transition metals for Mn [12, 13], small Rh and Co additions in LT-MnBi stabilize the orthorhombic phase whose structural and magnetic properties are close to those of the QHTP-$Mn_{1.08}$Bi high-temperature phase [14, 15].

Asymmetry in chemical mixing at the interface between Bi with Mn at the synthesis of LT-MnBi films is observed depending on the sequence of deposited layers [7, 10]. At the successive deposition of the first Mn layer on the substrate and the second Bi layer (Bi/Mn samples), the synthesis of LT-MnBi in a temperature range of 225–350°C requires three days (Williams method) [10, 16]. However, the 1-h annealing of Bi/Mn films did not lead to the formation of the LT-MnBi phase; instead, the formation of Mn clusters in the Bi matrix was observed [17]. In contrast to Bi/Mn samples, in Mn/Bi samples where the Bi layer is first deposited and the Mn layer is then deposited (Chen's method), even several minutes are sufficient for the synthesis of highly oriented LT-MnBi(001) films after annealing at ~300°C [7]. In this method, the oriented Bi(001) layer with the **c** axis perpendicular to the plane of the film growing on certain substrates is used. The deposition of the upper Mn layer initiates the migration of Mn atoms in the process of annealing at ~300°C to the Bi layer with the inheritance of the (001) orientation in the synthesized LT-MnBi phase. Chen's method is widely used to obtain and study LT-MnBi(001) films with a high per-

pendicular magnetic anisotropy $K_u \sim 10^6$ J/m^3, which is necessary for magnetic optical recording [5, 6], spintronics [18, 19], and thin-film magnets used in MEMS [20]. However, the nature of perpendicular magnetic anisotropy in MnBi films is still under discussion [21, 22].

The first studies of magnetic anisotropy in thin films showed that, in addition to classical types of magnetic anisotropies such as unidirectional, uniaxial (including perpendicular magnetic anisotropy), and magnetocrystalline, rotatable magnetic anisotropy exists in thin films. The fundamental difference of rotatable magnetic anisotropy from classical types of anisotropies is the rotation of the easy axis after the magnetic field [17]. Because of a high shape anisotropy in magnetically soft film samples, rotatable magnetic anisotropy was observed only in the plane of films. High rotatable magnetic anisotropy exceeding the shape anisotropy was first detected in magnetically hard MnGa [23] and CoPt [24] films. The easy axis in such samples can be arranged in any spatial direction by the magnetic field both in the plane of the film and perpendicular to it.

In this work, we report the first observation of high rotatable magnetic anisotropy in MnBi films. It is shown that, in addition to the well-studied oriented LT-MnBi(001) phase, which has high perpendicular magnetic anisotropy $K_u \sim 1\times10^7$ erg/cm^{-3}, a high rotatable magnetic anisotropy exceeding the film shape anisotropy can exist in polycrystalline LT-MnBi films.

SAMPLES AND EXPERIMENTAL PROCEDURE

In our experiments, we used Bi/Mn/Bi and Mn/Bi/Mn films obtained by thermal deposition of Mn and Bi layers on glass substrates in a vacuum of 10^{-6} Torr. The deposition of Mn and Bi layers with approximate stoichiometry Mn : Bi = 1 : 1 and a total thickness of 380 nm was performed at temperatures below 100°C. The initial Bi(140 nm)/Mn(100 nm)/Bi(140 nm) and Mn(50 nm)/Bi(280 nm)/Mn(50 nm) samples were annealed in a vacuum of 10^{-6} Torr at a temperature of 270°C for an hour. A temperature of 270°C is the optimal temperature for synthesis of LT-MnBi films. The appearing phases were identified on a DRON-4-07 diffractometer (CuK_α radiation). The samples for transmission electron microscopy were prepared by the cross-section method using a focused ion beam system (FIB, Hitachi FB2100). The electron microscopy studies were performed on a transmission electron microscope (Hitachi HT7700 at 100 kV, W source) equipped with a scanning transmission electron microscopy system (diameter of an electron probe was ~30 nm) and an energy dispersive X-ray spectrometer (Bruker Nano XFlash 6T/60). The saturation magnetization M_S and coercivity H_C were measured on a vibration magnetometer in magnetic fields up to 20 kOe. The saturation magnetization M_S was measured as a function of the temperature on an MPMS-XL SQUID magnetometer (Quantum Design) in a magnetic field of 5 kOe. Torque curves were recorded on a torque magnetometer with a maximum magnetic field of 12 kOe.

EXPERIMENTAL RESULTS FOR THE Bi/Mn/Bi FILM

Figure 1a shows the diffraction pattern of the Bi/Mn/Bi sample after annealing at a temperature of 270°C. Strong LT-MnBi(002) and LT-MnBi(004) peaks, as well as the absence of reflections from other phases, indicate the complete mixing of Mn and Bi layers and the synthesis of LT-MnBi(001) crystallites with the **c** axis perpendicular to the plane of the substrate. The diffraction pattern contains a weak Bi(012) peak, which demonstrates that an insignificant amount of unreacted bismuth is present in the sample. The electron microscopy studies and energy dispersive X-ray scans over the thickness show that Mn and Bi

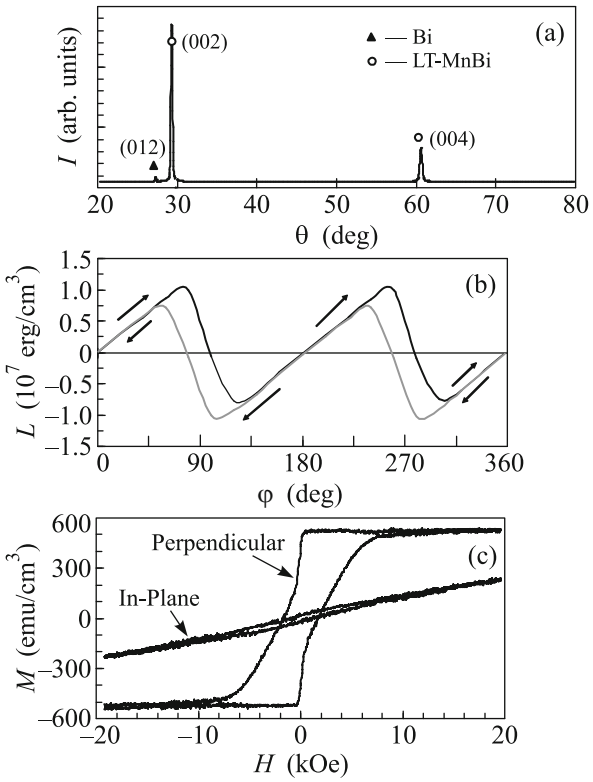

Fig. 1. (a) Diffraction pattern. (b) Torque curves $L_\perp(\varphi)$ at the rotation of the magnetic field $H = 12$ kOe by 360° from the easy axis perpendicular to the film (direct and inverse passes). (c) M–H hysteresis loops in the plane of the Bi/Mn/Bi film system and perpendicular to this plane after annealing at 270°C.

atoms are uniformly distributed over the entire thickness of the sample with the atomic ratio Mn : Bi = 50 : 50 corresponding to the LT-MnBi phase (they are not reported in this work). This result is in good agreement with the studies on the torque magnetometer, which indicate that the LT-MnBi(001) samples after annealing at 270°C had the easy axis perpendicular to the plane of the substrate (see Fig. 1b). The saturation magnetization M_S (see Fig. 1c) and perpendicular anisotropy field H_K after annealing at 270°C were $M_S = 520$ emu/cm^3 and $H_K = (43 \pm 2)$ kOe, respectively (see Fig. 1c). The saturation magnetization M_S is close to a value known for perfect LT-MnBi thin films [25, 26]. The perpendicular magnetic anisotropy constant $K_u = 1.1\times10^7$ erg/cm^3 was determined from the relation $H_K = 2K_u/M_S$, where $K_u = K_1 - 2\pi M_S^2$ (K_1 is the first constant of magnetic crystallographic anisotropy of the LT-MnBi phase and $2\pi M_S^2$ is the film shape anisotropy). This value is close to values obtained from the torque curve (see Fig. 1b) and from [17, 25, 26]. The reported results certainly prove that the synthesis of the highly oriented LT-MnBi(001) phase in Bi/Mn/Bi films is similar to Chen's method in Mn/Bi samples. For this reason, the structural and magnetic properties of LT-MnBi(001) films are identical in the Bi/Mn/Bi and Mn/Bi samples.

EXPERIMENTAL RESULTS FOR THE Mn/Bi/Mn FILMS

The sequence of Bi and Mn layers strongly affects the formation of MnBi nanostructures in the products of the reaction. Figure 2a shows the diffraction pattern of Mn/Bi/Mn films after annealing at a temperature of 270°C, where peaks from the LT-MnBi polycrystalline phase, as well as small peals from unreacted bismuth, are seen. Electron microscopy studies and energy dispersive X-ray linear scans over the thickness show that Mn and Bi layers reacted with an atomic ratio of Mn : Bi = 50 : 50 (they are not presented in this work). Figure 2 shows the direct, 0°–720°, and inverse, 720°–0°, passes of the torque curves (b) $L_\parallel$ and (c) $L_\perp$ in the plane of the Mn/Bi/Mn film and perpendicular to this plane, respectively, after annealing at 270°C. The torque curves $L_\parallel$ and $L_\perp$ have a large rotation hysteresis, which is a characteristic of rotatable magnetic anisotropy. Rotatable magnetic anisotropy was quantitatively characterized in [24] by the rotatable magnetic anisotropy constant $L_\parallel^{rot}$ for torque curves in the plane of the film, which was defined as the shift of the torque curves at the clockwise ($+L_\parallel^{rot}$) and counterclockwise ($-L_\parallel^{rot}$) rotations of the magnetic field (see Fig. 2b). The constants $+L_\perp^{rot}$ and $-L_\perp^{rot}$ for torque curves recorded in the direction perpendicular to the plane of the film at the clockwise and counterclockwise rotations, respectively, are defined similarly (see Fig. 2c). The experimental values of the rotatable magnetic anisotropy constants measured in the plane of the film and in the direction perpendicular to the plane of the film satisfy the relations $L_\parallel^{rot} = +L_\parallel^{rot} = -L_\parallel^{rot}$ and $L_\perp^{rot} = +L_\perp^{rot} = -L_\perp^{rot}$, respectively. The torque curves measured in the direction perpendicular to the plane of the film contain rotatable magnetic anisotropy with the constant $L_\perp^{rot} = 1.6\times10^6$ erg/cm^3 and a contribution from uniaxial anisotropy $K_0 \sin 2\varphi$ ($K_0 = 0.5\times10^6$ erg/cm^3) with the easy axis in the plane of the film. This implies that uniaxial anisotropy is determined by the film shape anisotropy $K_0 = 2\pi M_S^2$ with the saturation magnetization $M_S = 200$ emu/cm^3. However, this value is lower than the value $M_S = 350$ emu/cm^3, which follows from hysteresis loops (Fig. 3). This means that in-plane stresses and structural features, such as a columnar structure, reduce the parameter K_0.

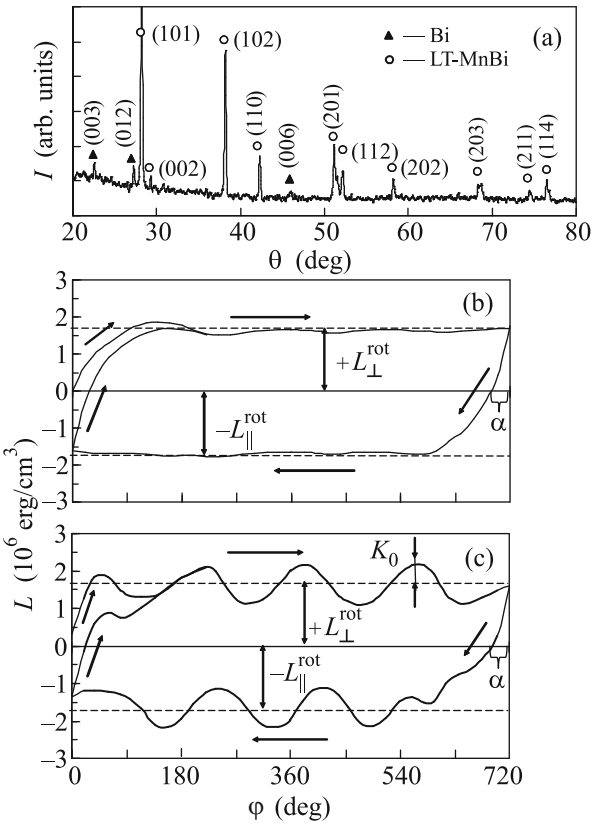

Fig. 2. (a) Diffraction pattern. (b, c) Torque curves $L_\parallel(\varphi)$ and $L_\perp(\varphi)$ at the rotation of the magnetic field $H = 12$ kOe in the plane of the Mn/Bi/Mn film system and perpendicular to this plane after annealing at 270°C, respectively, where α is the delay angle of the easy axis from the direction of the magnetic field.

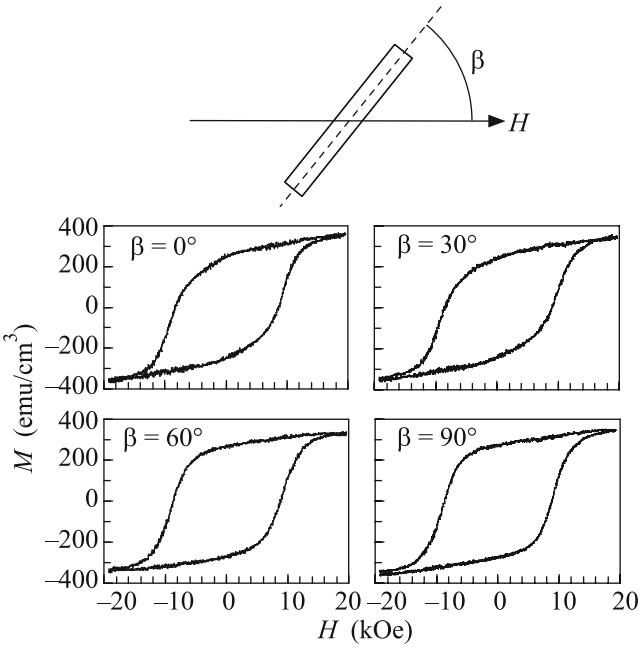

Fig. 3. M–H hysteresis loops at the angles β = 0°, 30°, 60°, and 90° to the plane of the Mn/Bi/Mn film system after annealing at 270°C.

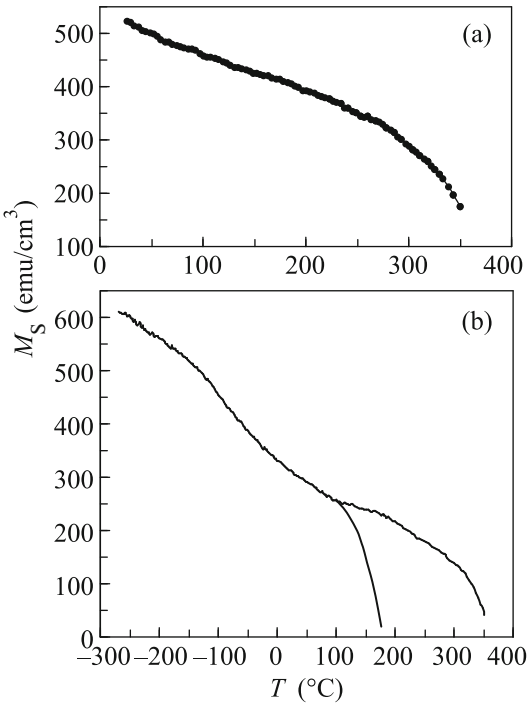

Fig. 4. Temperature dependences of the saturation magnetization M_S in the (a) LT-MnBi(001) and (b) (QHTP+LT)-MnBi films measured in a magnetic field of H = 5 kOe in the plane of the film.

It is remarkable that rotatable magnetic anisotropy constants in the plane $L_{\parallel}^{\text{rot}}$ and perpendicular to the plane $L_{\perp}^{\text{rot}}$ coincide with each other: $L_{\parallel}^{\text{rot}} = L_{\perp}^{\text{rot}} = 1.6\times10^6$ erg/cm^3. This equality, as well as the independence of hysteresis loops of the direction of the magnetic field (see Fig. 3), indicates the spatial isotropy of rotatable magnetic anisotropy. The inequality $L_{\parallel}^{\text{rot}} = L_{\perp}^{\text{rot}} > K_0$ is a necessary condition for the alignment of the easy axis by the magnetic field taking into account the delay angle α (see Figs. 2b and 2c) in an arbitrary direction in the plane and perpendicular to the plane of the film. The spatial isotropy of rotatable magnetic anisotropy was also observed in epitaxial $L1_0$CoPt(111) [24] and polycrystalline δ-$Mn_{0.6}Ga_{0.4}$ [23] films and implies a common nature of rotatable magnetic anisotropy in these samples.

DISCUSSION OF THE RESULTS

Although the total thicknesses of Mn and Bi layers were the same in Bi/Mn/Bi and Mn/Bi/Mn films and these films were annealed under the same conditions, they had a large difference in the structural and magnetic properties. The annealing of Bi/Mn/Bi films led to the expected synthesis of oriented LT-MnBi(001) films. The formation of LT-MnBi polycrystalline films with rotatable magnetic anisotropy after the annealing of the Mn/Bi/Mn film system clearly indicates the presence of transient layers at the Bi/Mn interface. It is known that the oxidation of Mn provides a negative effect and is responsible for change in the structural and magnetic properties in MnBi nanoparticles [27, 28] and thin films [7, 17, 29, 30]. In the Williams method, where a Mn layer is first deposited, oxygen contaminants form a diffusion barrier consisting of a chemisorbed layer or oxides on the surface of the Mn film, which suppresses the solid-phase reaction between the Mn and Bi layers. For this reason, the deposition of Bi on the oxidized Mn surface results in the formation of only polycrystalline layers in Bi/Mn and Mn/Bi/Mn samples. In contrast to Bi/Mn/Bi samples, the reaction in Mn/Bi/Mn samples starts between the Bi film and upper Mn layer with the formation of a LT-MnBi polycrystalline layer. The lower Mn layer simultaneously reacts with remaining Bi in the LT-MnBi layer without a significant change in its polycrystalline structure.

For a further analysis of ferromagnetic phases formed after annealing at 270°C in Bi/Mn/Bi and Mn/Bi/Mn films, we recorded the temperature dependences of saturation magnetization. The dependence $M_S(T)$ shown in Fig. 4a demonstrates that only the LT-MnBi phase with the Curie temperature $T_C \sim 360$°C is present in Bi/Mn/Bi samples. In Mn/Bi/Mn films, in addition to the LT-MnBi phase, a phase with the Curie temperature $T_C \sim 170$°C, which is characteristic of the QHTP-$Mn_{1.08}$Bi phase,

appears (see Fig. 4b). The volume fraction of the QHTP-$Mn_{1.08}Bi$ phase is roughly estimated from Fig. 4b as ~60%. However, reflections determined from Fig. 2a do not correspond to the QHTP-$Mn_{1.08}Bi$ orthorhombic phase (JPCD card 04-007-0814). The analysis performed in [31] showed that the QHTP-$Mn_{1.08}Bi$ phase can have a hexagonal or superlattice structure depending on the method of production. Our results are in good agreement with [32], where no changes in the lattice parameters were detected in films containing the LT-MnBi(001) phase and the mixture of the QHTP-$Mn_{1.08}Bi$ + LT-MnBi phases. In the process of QHTP $\rightleftarrows$ LT phase transitions, the lattice parameters vary continuously [8, 9], implying a common boundary of coherent coupling of QHTP-$Mn_{1.08}Bi$ and LT-MnBi lattices. For this reason, we assume that Mn/Bi/Mn polycrystalline films after annealing at 270°C consist of epitaxially coupled nanograins with close lattice parameters of the QHTP-$Mn_{1.08}Bi$ and LT-MnBi phases. This is in agreement with the fact that (QHTP+LT)-MnBi samples had a saturation magnetization of M_S = 350 emu/cm^3 (see Fig. 3), which is lower than the value M_S = 520 emu/cm^3 for LT-MnBi films (see Fig. 1c). The reason is that the saturation magnetization of QHTP-$Mn_{1.08}Bi$ is 75% of M_S for LT-MnBi films [7]. Furthermore, the coercivity of the (QHTP+LT)-MnBi samples (see Fig. 3) is sixfold higher than that of LT-MnBi samples (see Fig. 1c). This conclusion is consistent with the higher coercivity and lower saturation magnetization of the QHTP-$Mn_{1.08}Bi$ phase than the LT-MnBi phase [33].

It is noteworthy that oxygen and other contaminants in the process of annealing can dope the MnBi film and stabilize QHTP-$Mn_{1.08}Bi$ and other metastable phases. The constant L^{rot} in magnetically hard films depends on the composition and annealing conditions [34, 35]. A high rotatable magnetic anisotropy was observed in composite films containing a nanoscale mixture of two phases [24, 34, 35]. A great amount of attention has recently been focused on the fundamental understanding of the effect of nanoscale interfaces on the macroscopic properties of functional materials. Materials that include interacting phases and have a large fraction of interfaces can have unusual physical properties uncharacteristic of initial phases [36–38]. Consequently, it can be assumed that the structural coexistence of chemically coupled LT-MnBi and QHTP-$Mn_{1.08}Bi$ phases is energetically favorable under certain conditions and is important for the formation and nature of rotatable magnetic anisotropy.

CONCLUSIONS

The structural and magnetic asymmetry of phase transformations in Bi/Mn/Bi and Mn/Bi/Mn trilayer films has been studied near the equiatomic composition at an annealing temperature of 270°C. The annealing of Bi/Mn/Bi films has resulted in the formation of the highly oriented LT-MnBi(001) phase with the perpendicular magnetic anisotropy $K_u \sim 1.1\times10^7$ erg/cm^3 and coercivity $H_C \sim 1.5$ kOe. The annealing of Mn/Bi/Mn films under the same conditions has led to the formation of spatially isotropic nanoclusters ($H_C \sim 9.0$ kOe), which contain the main magnetically hard LT-MnBi phase epitaxially coupled with the QHTP-$Mn_{1.08}Bi$ phase. A high rotatable magnetic anisotropy has been detected in these films: the easy axis of anisotropy with the inclusion of the delay angle in magnetic fields above the coercivity $H > H_C$ can be oriented in any spatial direction. It has been assumed that the structural coexistence of LT-MnBi and QHTP-$Mn_{1.08}Bi$ phases is the main reason for the formation of rotatable magnetic anisotropy in Mn/Bi/Mn films. The high rotatable magnetic anisotropy detected in magnetically hard film materials assumingly allows the existence of a new class of ferromagnetic film media with the spatially tunable easy axis.

This work was supported by the Russian Foundation for Basic Research (project nos. 15-02-00948 and 16-03-00069), in part jointly by the Government of the Krasnoyarsk region and by the Russian Foundation for Basic Research (project no. 16-42-243006), by the Council of the President of the Russian Federation for Support of Young Scientists and Leading Scientific Schools (project no. SP-1373.2016.3), and by the Foundation for Promotion of the Development of Small Scientific and Engineering Enterprises (project no. 6650gu/2015, program Umnik). The electron microscopy studies were performed on the equipment of the Shared Usage Center, Krasnoyarsk Research Center, Siberian Branch, Russian Academy of Sciences.

REFERENCES

1. J. Shen, H. Cui, X. Huang, M. Gong, W. Qin, A. Kirkeminde, J. Cui, and S. Ren, RSC Adv. **5**, 5567 (2015).
2. N. Poudyal and J. P. Liu, J. Phys. D: Appl. Phys. **46**, 043001 (2013).
3. J. M. D. Coey, Scripta Mater **67**, 524 (2012).
4. N. V. Rama Rao, A. M. Gabay, and G. C. Hadjipanayis, J. Phys. D: Appl. Phys. **46**, 062001 (2013).
5. J. Köhler and J. Kübler, J. Phys.: Condens. Matter **8**, 8681 (1996).
6. Y. J. Wang, J. Magn. Magn. Mater. **84**, 39 (1990).
7. D. Chen, J. Appl. Phys. **42**, 3625 (1971).
8. H. Haudek and W. K. Unger, Phys. Status Solidi A **7**, 393 (1971).
9. K. Yoshida, T. Yamada, and Y. Furukawa, Acta Metallurg. **34**, 969 (1986).

10. Y. Iwama and Y. Takeno, Phys. Status Solidi A **76**, 75 (1983).
11. K. Yoshida and T. Yamada, Appl. Surf. Sci. **60–61,** 391 (1992).
12. J. Park, Y.-K. Hong, J. Lee, W. Lee, S.-G. Kim, and C.-J. Choi, Metals **4**, 455 (2014).
13. N. A. Zarkevich, L.-L. Wang, and D. D. Johnson, APL Mater. **2**, 032103 (2014).
14. V. Taufour, S. Thimmaiah, S. March, S. Saunders, K. Sun, T. N. Lamichhane, M. J. Kramer, S. L. Bud'ko, and P. C. Canfield, Phys. Rev. Appl. **4**, 014021 (2015).
15. S. Thimmaiah, V. Taufour, S. Saunders, S. March, Y. Zhang, M. J. Kramer, P. C. Canfield, and G. J. Miller, Chem. Mater. **28**, 8484 (2016).
16. H. J. Williams, R. C. Sherwood, F. G. Foster, and E. M. Kelley, J. Appl. Phys. **28**, 1181 (1957).
17. V. G. Myagkov, L. E. Bykova, V. Yu. Yakovchuk, V. S. Zhigalov, M. N. Volochaev, V. A. Seredkin, A. A. Matsynin, I. A. Tambasov, G. S. Patrin, and G. N. Bondarenko, JETP Lett. **103**, 254 (2016).
18. P. Kharel, P. Thapa, P. Lukashev, R. F. Sabirianov, E. Y. Tsymbal, D. J. Sellmyer, and B. Nadgorny, Phys. Rev. B **83**, 024415 (2011).
19. K. Tarawneh, N. Al-Aqtash, and R. Sabirianov, J. Magn. Magn. Mater. **363**, 43 (2014).
20. M. R. J. Gibbs, E. W. Hill, and P. J. Wright, J. Phys. D: Appl. Phys. **37**, R237 (2004).
21. T. Suwa, Y. Tanaka, G. Mankey, R. Schad, and T. Suzuki, AIP Adv. **6**, 056008 (2016).
22. Y. Liu, L. Peng, J. Zhang, Z. Ren, J. Yang, Z. Yang, S. Cao, and W. Fang, Eur. Phys. Lett. **96**, 27015 (2011).
23. V. G. Myagkov, V. S. Zhigalov, L. E. Bykova, G. N. Bondarenko, Yu. L. Mikhlin, G. S. Patrin, and D. A. Velikanov, Phys. Status Solidi B **249**, 1541 (2012).
24. V. G. Myagkov, V. S. Zhigalov, L. E. Bykova, G. N. Bondarenko, D. A. Velikanov, A. N. Rybakova, A. A. Matsynin, I. A. Tambasov, and M. N. Volochaev, JETP Lett. **102**, 355 (2015).
25. M. Y. Sun, X. W. Xu, X. A. Liang, X. W. Sun, and Y. J. Zheng, J. Alloys Compd. **672**, 59 (2016).
26. T. Suwa, Y. Tanaka, G. Mankey, R. Schad, and T. Suzuki, AIP Adv. **6**, 056008 (2016).
27. K. Kanari, C. Sarafidis, M. Gjoka, D. Niarchos, and O. Kalogirou, J. Magn. Magn. Mater. **426**, 691 (2017).
28. J. Cui, J.-P. Choi, E. Polikarpov, M. E. Bowden, W. Xie, G. Li, Z. Nie, N. Zarkevich, and M. J. Kramer, Acta Mater. **79**, 374 (2014).
29. U. Deffke, G. Ctistis, J. J. Paggel, P. Fumagalli, U. Bloeck, and M. Giersig, J. Appl. Phys. **96**, 3972 (2004).
30. M. Y. Sun, X. W. Xu, X. A. Liang, X. W. Sun, and Y. J. Zheng, J. Alloys Compd. **672**, 59 (2016).
31. G. S. Xu, C. S. Lakshmi, and R. W. Smith, J. Mater. Sci. Lett. **8**, 1113 (1989).
32. Y. Kido and M. Tada, J. Mater. Res. **4**, 1151 (1989).
33. D. Chen and R. L. Aagard, J. Appl. Phys. **41**, 2530 (1971).
34. V. G. Myagkov, L. E. Bykova, V. S. Zhigalov, A. A. Matsynin, D. A. Velikanov, and G. N. Bondarenko, J. Alloys Compd. **706**, 38 (2017).
35. V. S. Zhigalov, V. G. Myagkov, L. E. Bykova, G. N. Bondarenko, A. A. Matsynin, and M. N. Volochaev, Phys. Solid State **59**, 392 (2017).
36. J. X. Zhang, R. J. Zeches, Q. He, Y.-H. Chu, and R. Ramesh, Nanoscale **4**, 6196 (2012).
37. Y. Lee and Z. Q. Liu, J. T. Heron, et al., Nat. Commun. **6**, 5959 (2015).
38. T. Ma, J. Gou, S. Hu, X. Liu, C. Wu, S. Ren, H. Zhao, A. Xiao, C. Jiang, X. Ren, and M. Yan, Nat. Commun. **8**, 13937 (2017).

Translated by R. Tyapaev